Screening strain sensitive transition metals using oxygen adsorption

Yucheng He, Pengqi Hai, Chao Wu*

Frontier Institute of Science and Technology, Xi'an Jiaotong University, Xi'an

710049, Shaanxi, People's Republic of China

*corresponding author at: Frontier Institute of Science and Technology, Xi'an

Jiaotong University, Xi'an 710049, Shaanxi, People's Republic of China

E-mail address: chaowu@xjtu.edu.cn

Contents
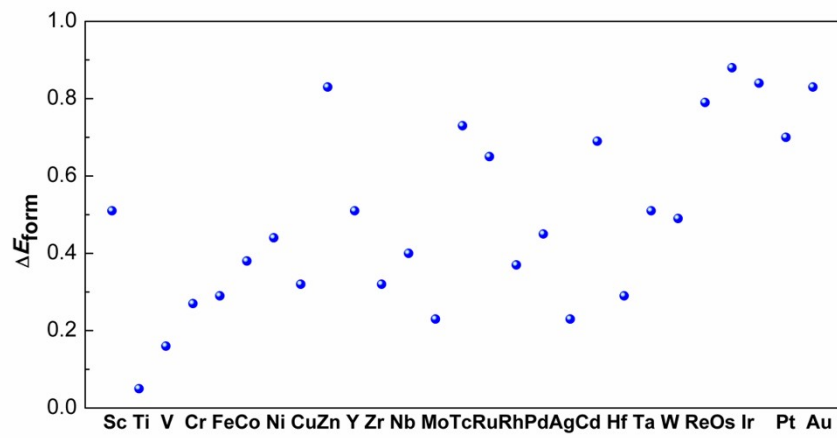
Figure S1.The absolute variation of the formation energy of isolated O* adatomsin the strain variation range(±5%).
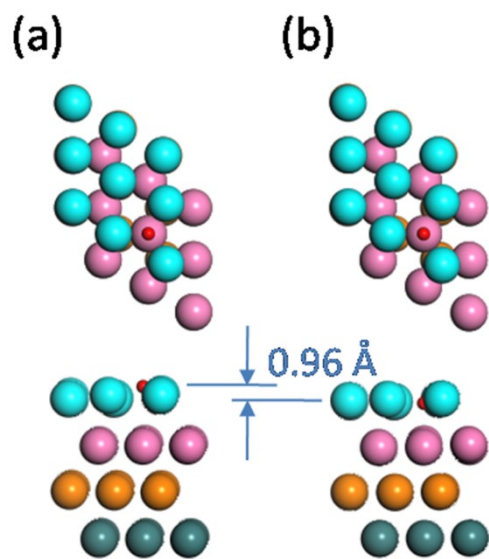
Figure S2. Top and side views of isolated O atom adsorbed on the Cd (0001) facet at (a) 2% stain, and (b) 3% strain. Large balls represent metal atoms and small red balls represent oxygen atom.
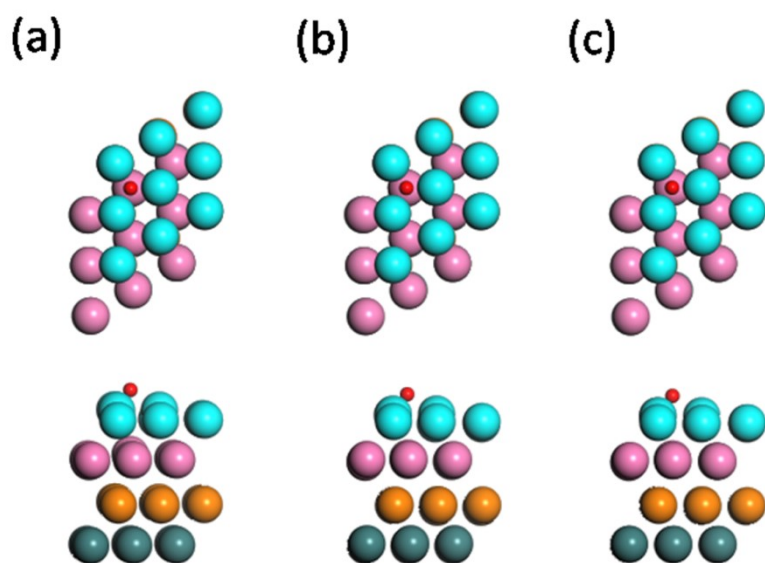
Figure S3. Top and side views of isolated O atom adsorbed on the Ti (0001) facet at (a) -4% stain, (b) -3% strain, and (c) -2% strain.
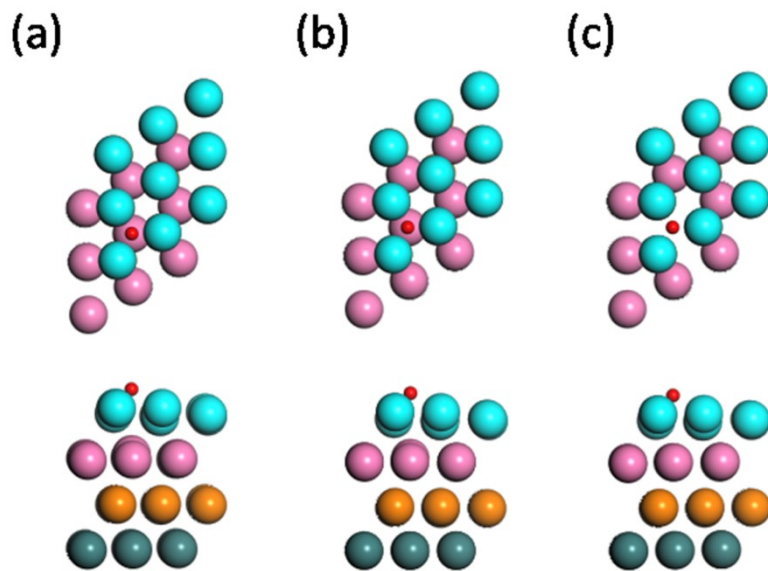
Figure S4.Top and side views of isolated O atom adsorbed on the Zr (0001) facet at (a) -4% stain, (b) -3% strain, and (c) -2% strain.
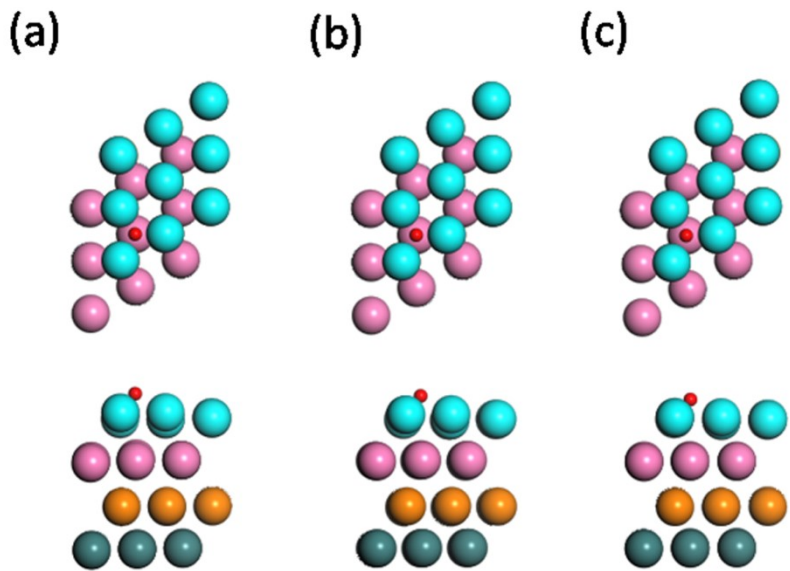
Figure S5.Top and side views of isolated O atom adsorbed on the Hf (0001) facet at (a) -4% stain, (b) -3% strain, and (c) -2% strain.
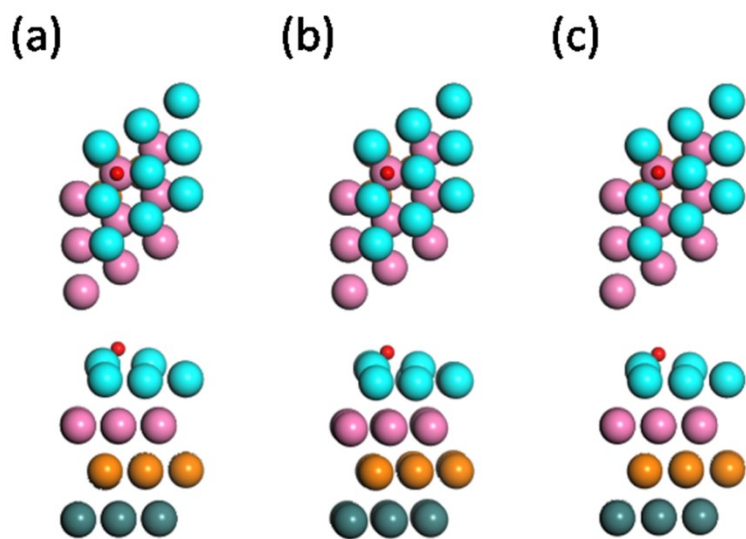
Figure S6.Top and side views of isolated O atom adsorbed on the Zn (0001) facet at (a) -4% stain, (b) -3% strain, and (c) -2% strain.
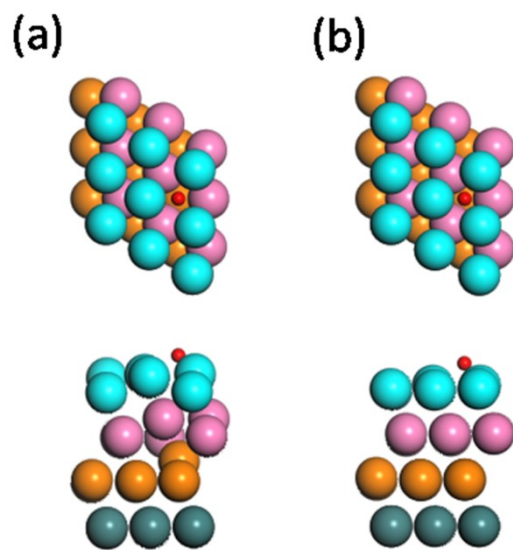
Figure S7.Top and side views of isolated O atom adsorbed on the Au (111) facet at (a) -5% stain, and (b) -4% strain.
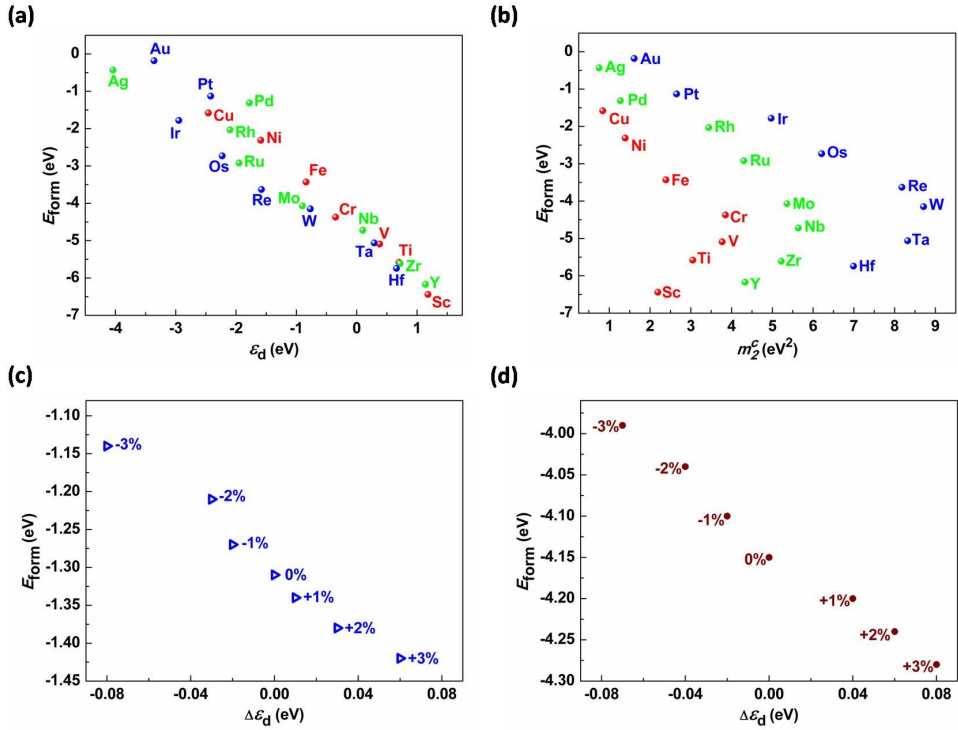
Figure S8. Formation energy of two 1NN O*adatoms on unstrained close-packed metal facets as a function of (a) the *d*-band center ε_d and (b) the second moment of electronic density of states distribution m_2^c. Formation energy of two 1NN O*adatoms on (c) Pd(111) and (d) W(110) as a function of the *d*-band center shift $\Delta\varepsilon_d$. The ε_d (in a) and m_2^c (in b) are taken from the work of Nørskov et al.[1] The numbers (in c and d) represent the applied strain.
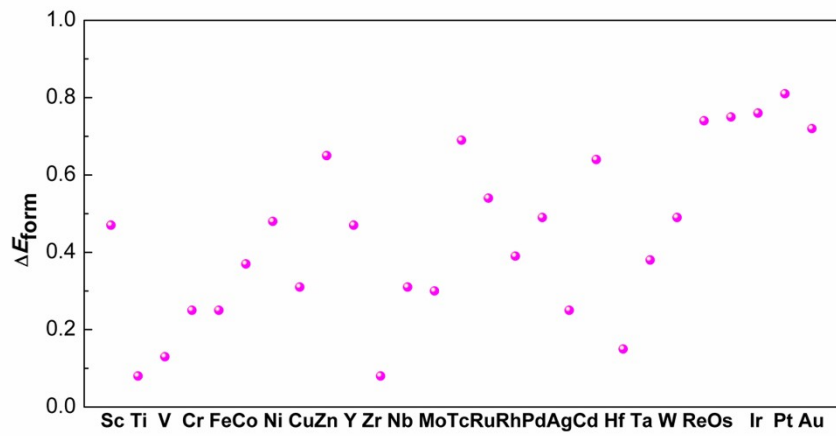
Figure S9.The absolute variation of the formation energy of two1NN O* adatomsin the strain variation range(±5%).
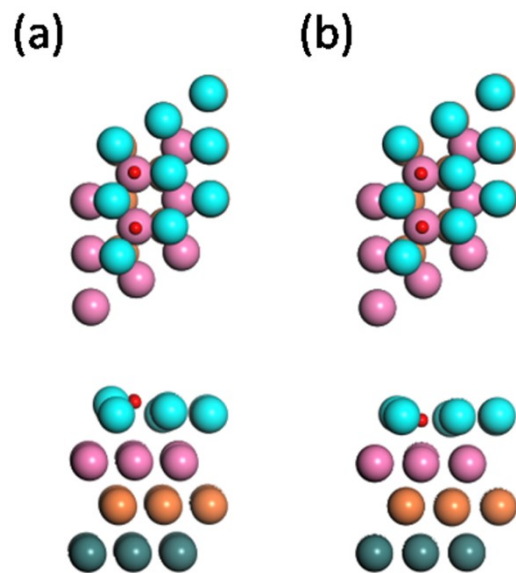
Figure S10. Top and side views of two 1NN O atoms adsorbed on the Cd (0001) facet at (a) +3% stain, and (b) +4% strain.
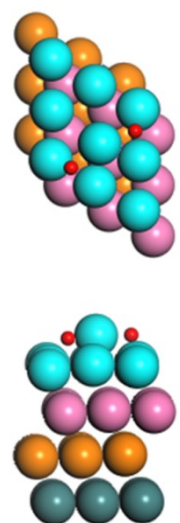
Figure S11. Top and side views of two 1NN O atoms adsorbed on the Ag (111) facet at -5% strain.
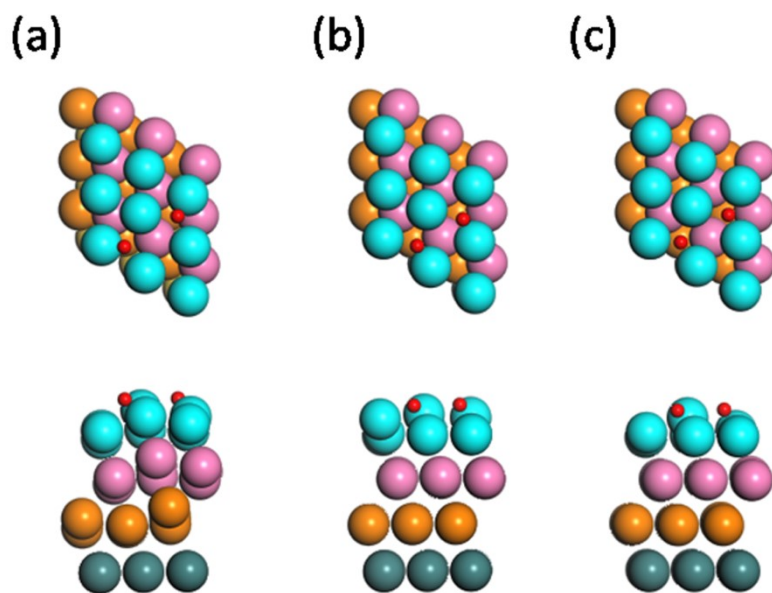
Figure S12. Top and side views of two 1NN O atoms adsorbed on the Au (111) facet at (a) -5% stain, (b) -4% strain, and (c) -3% strain.
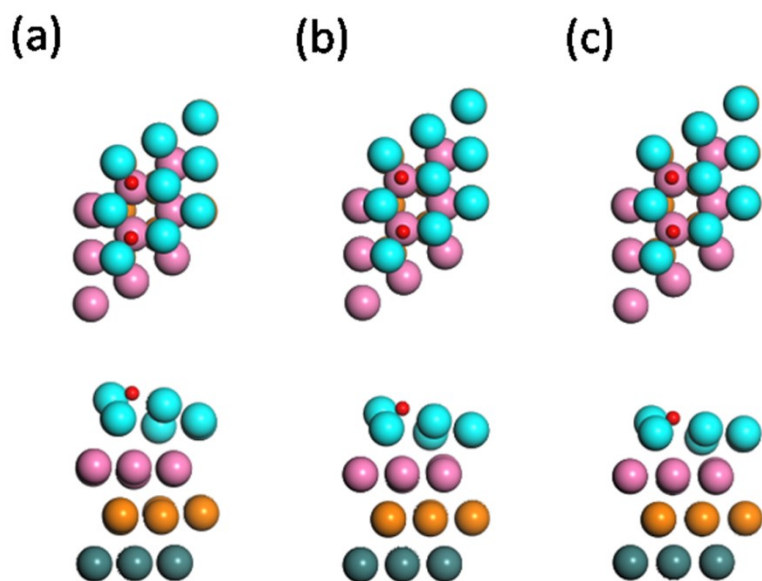
Figure S13. Top and side views of two 1NN O atoms adsorbed on the Zn (0001) facet at (a) -4% stain, (b) 0% strain, and (c) +4% strain.
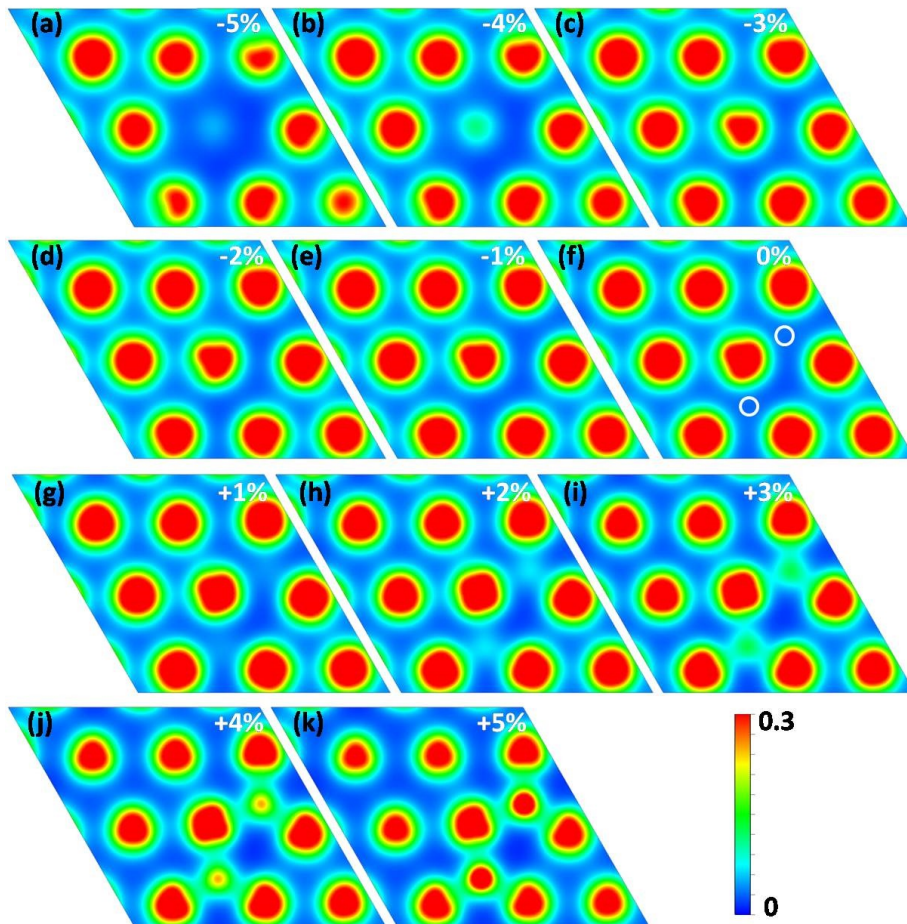
Figure S14.Slices of electron density plots of two 1NN O atoms adsorbed on Pt(111) under the strain (ranging from -5% to +5%). The corresponding strain values are marked in (a) – (k). The white cycles in (f) denote the projected sites of two O* adatoms. The normal direction of slice is [001] of slab model and z= 6.96 Åwhich is the vertical position of surface Pt atoms of O-free and unstrained Pt(111).The electron density shape of Pt atom sandwiched by two O atoms changes obviously with the applied strain, the trend of which is consistent with the variation of E_{form}. The spherical symmetric electron density of Pt atoms away from two O* adatoms is reversed from -5% to +1% strain, while electron density of Pt atoms adjacent to two O* adatoms is not symmetric within the whole strain range.The variation of electron density indicates that due to O atoms adsorption, all surface Pt atoms could not correspond to the global strain uniformly.
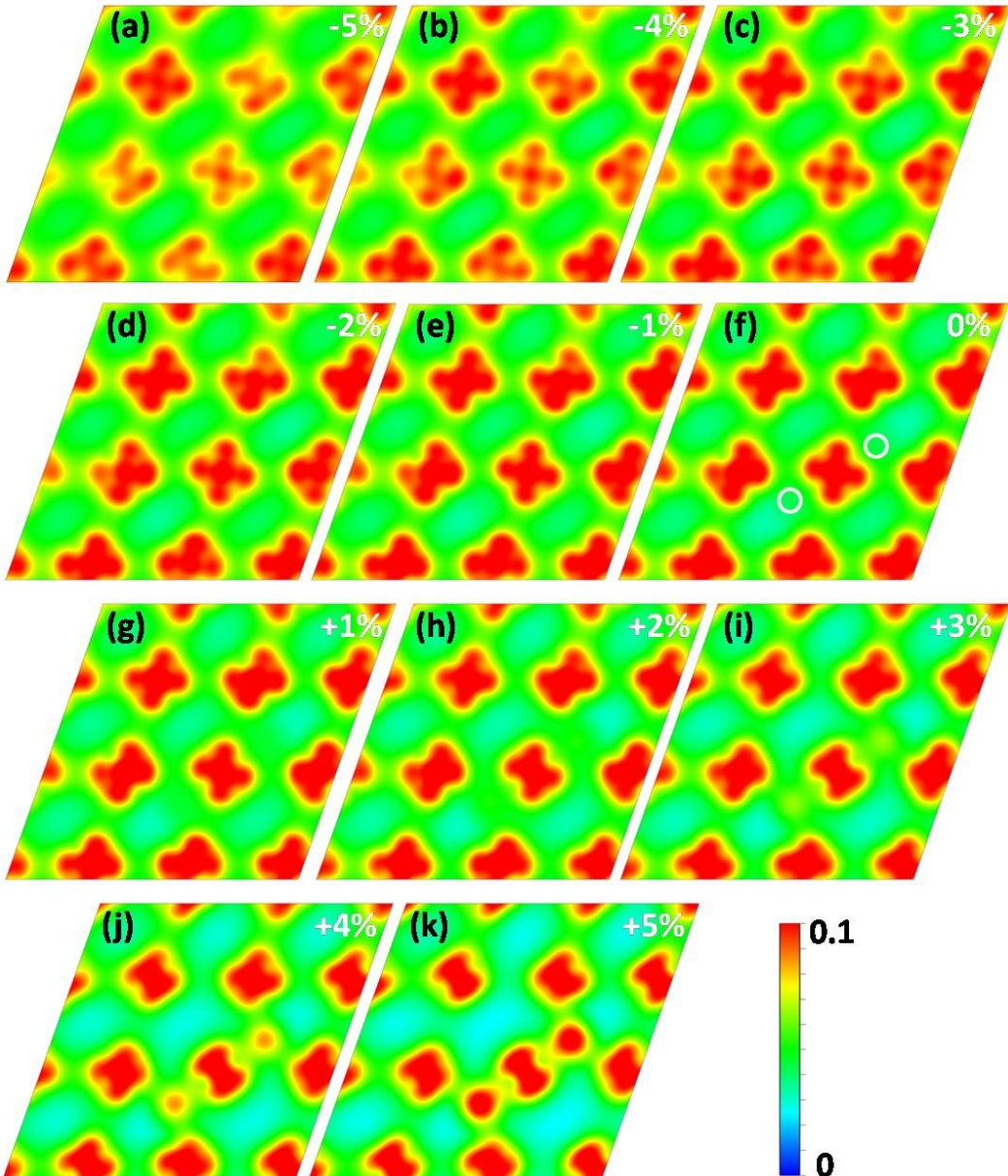
Figure S15. Slices of electron density plots of two 1NN O atoms adsorbed on W(110) under the strain (ranging from -5% to +5%). The corresponding strain values are marked in (a) – (k). The white cycles in (f) denote the projected sites of two O* adatoms. The normal direction of slice is [001] of slab model and z= 6.64 Å,which is the vertical position of surface W atoms of O-free and unstrained W(110). The electron distribution of density and shapeof each W atom is almost similar to one another under the same strain, which indicates that all surface W atoms follow form the strain variation in a similar fashion.
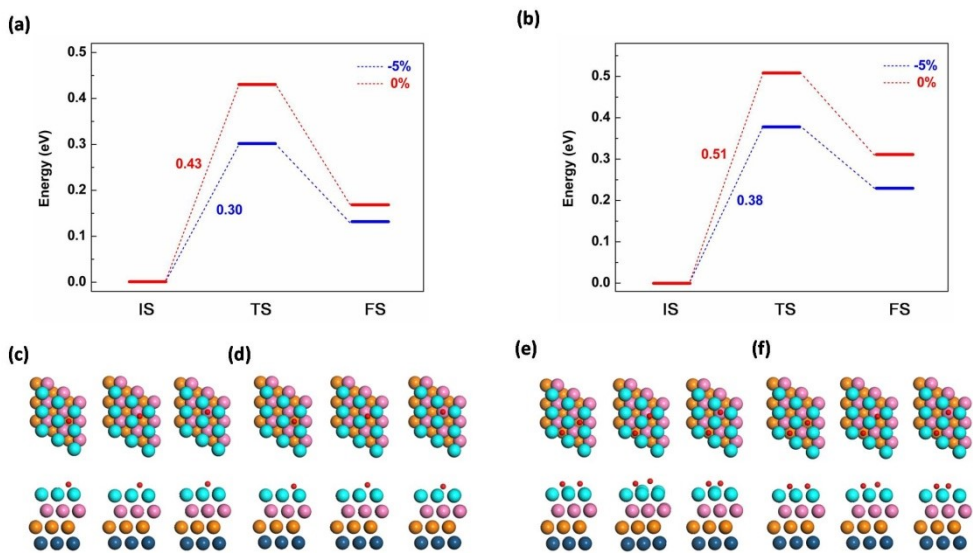
Figure S16. O* adatom diffusion on Ir(111). Energy profiles over (a) isolated-O* model and (b) double-O* model. (c), (d), (e) and (f) Key structures of the O* adatom diffusion. The panels are the top view, the bottom panels are the side view.

Table S1 Comparison between PW91 and PBE functionals (eV)

Model	Strain	E_{form}		ΔE_{form}		$\Delta E_{\text{form}}\%$	
		PW91	PBE	PW91	PBE	PW91	PBE
Ir Isolated-O*	-5%	-1.57	-1.50				
	0%	-1.82	-1.74	0.84	0.81	46%	47%
	5%	-2.41	-2.31				
Ir Double-O*	-5%	-1.49	-1.40				
	0%	-1.78	-1.69	0.76	0.74	43%	44%
	5%	-2.25	-2.15				
Pt Isolated-O*	-5%	-0.91	-0.80				
	0%	-1.22	-1.11	0.70	0.71	57%	64%
	5%	-1.61	-1.51				
Pt Double-O*	-5%	-0.75	-0.64				
	0%	-1.13	-1.03	0.80	0.82	71%	80%
	5%	-1.55	-1.46				

Table S2 Effect of dispersion correction on formation energy (eV)

Model	Strain	E_{form}	E_{dip}	ΔE_{form}	ΔE_{form}-D3	$\Delta E_{form}\%$	$\Delta E_{form}\%$-D3
Ir Isolated-O*	-5%	-1.57	-0.16				
	0%	-1.82	-0.15	0.84	0.88	46%	45%
	5%	-2.41	-0.19				
Ir Double-O*	-5%	-1.49	-0.15				
	0%	-1.78	-0.15	0.76	0.79	43%	41%
	5%	-2.25	-0.18				
Pt Isolated-O*	-5%	-0.91	-0.13				
	0%	-1.22	-0.20	0.70	0.71	57%	50%
	5%	-1.61	-0.14				
Pt Double-O*	-5%	-0.75	-0.13				
	0%	-1.13	-0.21	0.80	0.83	71%	62%
	5%	-1.55	-0.16				

Table S3. Relative change of interplanar spacing between surface and 1st subsurface ($d_{sur-1^{st}sub}$).

Metal facet	Relative change of $d_{sur-1^{st}sub}$ under the strain (%)										
	-5%	-4%	-3%	-2%	-1%	0%	1%	2%	3%	4%	5%
Sc(0001)	5	4	3	2	1	0	-1	-2	-3	-3	-4
Ti(0001)	5	4	3	2	1	0	-1	-1	-2	-3	-3
V(110)	9	7	5	4	2	0	-1	-2	-4	-5	-6
Cr(110)	5	4	3	2	1	0	-1	-2	-3	-4	-5
Fe(110)	4	3	2	2	1	0	-1	-2	-2	-3	-4
Co(111)	4	3	2	1	1	0	-1	-1	-2	-3	-3
Ni(111)	4	3	3	2	1	0	0	-1	-2	-3	-3
Cu(111)	5	4	3	2	1	0	-1	-2	-2	-3	-4
Zn(0001)	4	2	2	1	1	0	-1	-1	-2	-2	-6
Y(0001)	3	2	2	1	0	0	-1	-1	-2	-3	-3
Zr(0001)	6	4	3	2	1	0	-1	-1	-2	-3	-3
Nb(110)	7	6	5	3	2	0	-1	-3	-4	-5	-6
Mo(110)	5	4	3	2	1	0	-1	-2	-3	-4	-5
Tc(0001)	3	2	2	1	0	0	-1	-1	-2	-3	-3
Ru(0001)	3	2	2	1	1	0	-1	-2	-2	-3	-4
Rh(111)	3	3	2	1	1	0	-1	-1	-2	-3	-3
Pd(111)	4	4	3	2	1	0	-1	-2	-3	-4	-5
Ag(111)	7	5	3	3	2	0	-1	-2	-3	-4	-5
Cd(0001)	3	2	2	2	0	0	0	-2	-2	-3	-6
Hf(0001)	3	3	2	1	1	0	-1	-1	-2	-2	-3
Ta(110)	7	5	4	3	1	0	-1	-2	-4	-5	-6
W(110)	5	4	3	2	1	0	-1	-2	-3	-4	-5
Re(0001)	4	2	2	1	1	0	-1	-1	-2	-3	-3
Os(0001)	3	3	2	2	1	0	-1	-1	-2	-3	-3
Ir(111)	3	2	2	1	1	0	-1	-1	-2	-3	-3
Pt(111)	5	4	3	2	1	0	-1	-3	-4	-5	-7
Au(111)	10	9	7	6	3	0	-1	-2	-4	-5	-6

Table S4. Formation energy of isolated O atom on the metal close-packed facet.

Metal facet	E_{form} of isolated O* (eV)										
	-5%	-4%	-3%	-2%	-1%	0%	1%	2%	3%	4%	5%
Sc(0001)	-6.14	-6.20	-6.27	-6.34	-6.40	-6.45	-6.50	-6.54	-6.57	-6.60	-6.65
Ti(0001)	-5.90	-5.80	-5.76	-5.69	-5.59	-5.56	-5.56	-5.55	-5.55	-5.57	-5.63
					-5.41[2]						
V(110)	-4.96	-5.03	-5.05	-5.07	-5.04	-5.07	-5.06	-5.05	-5.07	-5.11	-5.12
Cr(110)	-4.22	-4.25	-4.28	-4.35	-4.42	-4.47	-4.52	-4.55	-4.53	-4.50	-4.49
Fe(110)	-3.31	-3.34	-3.38	-3.41	-3.45	-3.50	-3.55	-3.56	-3.53	-3.51	-3.08
					-3.43[3]						
Co(111)	-2.43	-2.47	-2.51	-2.55	-2.59	-2.63	-2.65	-2.68	-2.72	-2.76	-2.80
	-2.25[4]										
Ni(111)	-2.22	-2.29	-2.35	-2.40	-2.45	-2.50	-2.53	-2.57	-2.60	-2.63	-2.66
					-5.90	-5.44[5]					
Cu(111)	-1.61	-1.61	-1.65	-1.72	-1.74	-1.78	-1.82	-1.85	-1.88	-1.90	-1.93
					-5.18	-4.80[6]					
Zn(0001)	-1.84	-1.80	-1.79	-1.83	-1.91	-2.04	-2.14	-2.25	-2.37	-2.50	-2.61
Y(0001)	-5.92	-5.98	-6.03	-6.09	-6.14	-6.20	-6.25	-6.30	-6.35	-6.39	-6.43
Zr(0001)	-5.84	-5.84	-5.76	-5.71	-5.64	-5.60	-5.58	-5.58	-5.56	-5.53	-5.52
					-9.00	-8.77[7]					
Nb(110)	-4.45	-4.52	-4.59	-4.63	-4.65	-4.69	-4.75	-4.77	-4.79	-4.82	-4.85
					-5.08[8]						
Mo(110)	-4.01	-4.02	-4.06	-4.10	-4.15	-4.18	-4.20	-4.21	-4.23	-4.24	-4.21
						-7.58	-7.35[9]				
Tc(0001)	-3.21	-3.28	-3.33	-3.40	-3.48	-3.58	-3.68	-3.77	-3.81	-3.88	-3.94
Ru(0001)	-2.67	-2.74	-2.81	-2.88	-2.95	-3.05	-3.13	-3.19	-3.25	-3.30	-3.31
					-2.71[10]						
Rh(111)	-1.99	-2.00	-2.02	-2.06	-2.10	-2.13	-2.16	-2.20	-2.24	-2.29	-2.36
					-5.53-5.22[11]						
Pd(111)	-1.14	-1.22	-1.28	-1.34	-1.38	-1.42	-1.46	-1.49	-1.51	-1.55	-1.59
					-1.48[12]						
Ag(111)	-0.49	-0.52	-0.52	-0.55	-0.60	-0.65	-0.68	-0.70	-0.69	-0.71	-0.72
	-4.05	-3.82[13]									
Cd(0001)	-1.25	-1.21	-1.23	-1.29	-1.36	-1.44	-1.54	-1.65	-1.81	-1.90	-1.94
Hf(0001)	-6.01	-5.86	-5.78	-5.74	-5.72	-5.73	-5.76	-5.80	-5.83	-5.86	-5.93
Ta(110)	-4.68	-4.77	-4.85	-4.94	-5.00	-5.04	-5.10	-5.17	-5.11	-5.14	-5.18
W(110)	-3.95	-4.02	-4.07	-4.14	-4.22	-4.29	-4.34	-4.37	-4.39	-4.43	-4.44
					-4.16[14]						
Re(0001)	-3.24	-3.27	-3.32	-3.41	-3.52	-3.63	-3.75	-3.88	-3.94	-3.97	-4.03
Os(0001)	-2.30	-2.38	-2.48	-2.62	-2.76	-2.82	-2.91	-3.00	-3.09	-3.14	-3.18
Ir(111)	-1.57	-1.62	-1.66	-1.72	-1.77	-1.82	-1.89	-1.96	-2.06	-2.22	-2.41
					-5.22-4.57[15]						
Pt(111)	-0.91	-0.92	-0.99	-1.06	-1.14	-1.22	-1.31	-1.43	-1.51	-1.58	-1.61

					-1.03[16]						
Au(111)	0.20	0.32	0.16	-0.04	-0.27	-0.35	-0.37	-0.42	-0.49	-0.51	-0.51
					-3.75-3.38[17]						

Formation energy E_{form} taking the energy of free oxygen atom as reference are represented in bold.

Table S5. Fitting line of the formation energy of isolated O*adatoms and the metal's valency.

Strain	Slope				Intercept		
	Period 4	Period 5	Period 6		Period 4	Period 5	Period 6
-5%	0.54	0.62	0.84		-7.67	-7.76	-9.09
-4%	0.54	0.63	0.84		-7.70	-7.83	-9.12
-3%	0.54	0.62	0.82		-7.72	-7.85	-9.03
-2%	0.53	0.62	0.80		-7.72	-7.86	-8.97
-1%	0.52	0.61	0.78		-7.69	-7.85	-8.90
0%	0.52	0.61	0.77		-7.67	-7.86	-8.91
1%	0.51	0.60	0.77		-7.67	-7.88	-8.97
2%	0.50	0.60	0.77		-7.65	-7.89	-9.01
3%	0.50	0.59	0.75		-7.62	-7.87	-8.95
4%	0.49	0.59	0.75		-7.60	-7.87	-8.96
5%	0.49	0.58	0.75		-7.58	-7.87	-9.01

Table S6. Formation energy of two1NN O*adatoms on close-packed metal facets.

Metal facet	E_{form} of two O* (eV)										
	-5%	-4%	-3%	-2%	-1%	0%	1%	2%	3%	4%	5%
Sc(0001)	-6.14	-6.21	-6.27	-6.34	-6.39	-6.44	-6.48	-6.52	-6.55	-6.58	-6.61
Ti(0001)	-5.66	-5.62	-5.62	-5.60	-5.58	-5.58	-5.58	-5.58	-5.59	-5.59	-5.61
V(110)	-4.99	-5.04	-5.07	-5.09	-5.08	-5.09	-5.09	-5.08	-5.09	-5.11	-5.12
Cr(110)	-4.18	-4.20	-4.24	-4.29	-4.33	-4.37	-4.41	-4.45	-4.44	-4.42	-4.42
Fe(110)	-3.23	-3.25	-3.32	-3.34	-3.39	-3.43	-3.46	-3.48	-3.45	-3.45	-3.38
Co(111)	-2.32	-2.35	-2.38	-2.41	-2.45	-2.48	-2.52	-2.56	-2.60	-2.64	-2.69
Ni(111)	-2.04	-2.09	-2.15	-2.20	-2.25	-2.31	-2.35	-2.40	-2.44	-2.48	-2.52
Cu(111)	-1.46	-1.47	-1.49	-1.51	-1.54	-1.58	-1.62	-1.66	-1.69	-1.73	-1.77
Zn(0001)	-1.90	-1.87	-1.86	-1.90	-1.96	-2.05	-2.13	-2.22	-2.32	-2.43	-2.51
Y(0001)	-5.91	-5.96	-6.01	-6.07	-6.12	-6.17	-6.21	-6.26	-6.30	-6.34	-6.38
Zr(0001)	-5.63	-5.67	-5.66	-5.65	-5.63	-5.61	-5.61	-5.61	-5.61	-5.60	-5.59
Nb(110)	-4.52	-4.57	-4.63	-4.66	-4.68	-4.72	-4.76	-4.78	-4.79	-4.80	-4.82
Mo(110)	-3.87	-3.89	-3.93	-3.98	-4.03	-4.07	-4.11	-4.14	-4.16	-4.17	-4.16
Tc(0001)	-3.18	-3.24	-3.29	-3.36	-3.44	-3.52	-3.61	-3.69	-3.75	-3.81	-3.87
Ru(0001)	-2.58	-2.65	-2.71	-2.78	-2.84	-2.92	-2.98	-3.03	-3.07	-3.10	-3.11
Rh(111)	-1.85	-1.88	-1.92	-1.96	-2.00	-2.03	-2.07	-2.11	-2.15	-2.19	-2.24
Pd(111)	-1.01	-1.07	-1.14	-1.21	-1.27	-1.31	-1.34	-1.38	-1.42	-1.46	-1.50
Ag(111)	-0.39	-0.35	-0.33	-0.34	-0.39	-0.43	-0.46	-0.49	-0.51	-0.55	-0.58
Cd(0001)	-1.28	-1.24	-1.26	-1.31	-1.36	-1.44	-1.52	-1.60	-1.68	-1.82	-1.88
Hf(0001)	-5.84	-5.78	-5.75	-5.74	-5.74	-5.74	-5.76	-5.78	-5.81	-5.84	-5.88
Ta(110)	-4.75	-4.84	-4.91	-4.98	-5.03	-5.06	-5.09	-5.13	-5.11	-5.11	-5.13
W(110)	-3.86	-3.93	-3.99	-4.04	-4.10	-4.15	-4.20	-4.24	-4.28	-4.32	-4.35
Re(0001)	-3.25	-3.28	-3.33	-3.42	-3.52	-3.63	-3.73	-3.85	-3.91	-3.94	-3.99
Os(0001)	-2.28	-2.36	-2.45	-2.57	-2.67	-2.73	-2.80	-2.88	-2.95	-2.99	-3.02
Ir(111)	-1.49	-1.54	-1.60	-1.66	-1.72	-1.78	-1.83	-1.89	-1.98	-2.11	-2.25
Pt(111)	-0.75	-0.77	-0.84	-0.93	-1.03	-1.13	-1.23	-1.34	-1.43	-1.50	-1.55
Au(111)	0.27	0.22	0.17	0.04	-0.11	-0.18	-0.22	-0.29	-0.37	-0.42	-0.45

Table S7. Fitting line of the formation energy of two 1NN O*adatoms and the metal's valency.

Strain	Slope				Intercept		
	Period 4	Period 5	Period 6		Period 4	Period 5	Period 6
-5%	0.54	0.62	0.84		-7.60	-7.68	-9.07
-4%	0.54	0.63	0.84		-7.64	-7.77	-9.07
-3%	0.54	0.63	0.83		-7.69	-7.82	-9.07
-2%	0.54	0.63	0.82		-7.72	-7.85	-9.05
-1%	0.54	0.63	0.80		-7.72	-7.87	-9.01
0%	0.53	0.62	0.79		-7.72	-7.89	-8.99
1%	0.53	0.62	0.79		-7.71	-7.91	-9.01
2%	0.52	0.62	0.78		-7.70	-7.92	-9.01
3%	0.51	0.61	0.77		-7.68	-7.93	-8.97
4%	0.51	0.60	0.76		-7.65	-7.90	-8.95
5%	0.50	0.60	0.75		-7.64	-7.90	-8.97

Table S8 Comparison between formation energy and free energy (eV)

Model	Strain	E_{form}	ΔZPE-$T\Delta S$	ΔE_{form}	ΔG	$\Delta E_{\text{form}}\%$	$\Delta G\%$
Ir Isolated-O*	-5%	-1.57	0.20				
	0%	-1.82	0.14	0.84	0.88	46%	53%
	5%	-2.41	0.15				
Ir Double-O*	-5%	-1.49	0.21				
	0%	-1.78	0.27	0.76	0.81	43%	54%
	5%	-2.25	0.16				
Pt Isolated-O*	-5%	-0.91	0.15				
	0%	-1.22	0.11	0.70	0.77	57%	69%
	5%	-1.61	0.08				
Pt Double-O*	-5%	-0.75	0.16				
	0%	-1.13	0.14	0.80	0.84	71%	84%
	5%	-1.55	0.13				

References:

1 A. Vojvodic, J. K. Nørskov and F. Abild-Pedersen, *Topics in Catal.*, 2013, **57**, 25-32.

2 J. Liu, X. Fan, C. Sun and W. Zhu, *RSC Adv.*, 2016, **6**, 71311-71318.

3 S. Liu, X. Tian, T. Wang, X. Wen, Y.-W. Li, J. Wang and H. Jiao, *Phys. Chem. Chem. Phys.*, 2015, **17**, 8811-8821.

4 S. H. Ma, Z. Y. Jiao, T. X. Wang and X. Q. Dai, *Euro. Phys. J. B*, 2015, **88**, 4.

5 N. K. Das and T. Shoji, *Appl. Surf. Sci.*, 2018, **445**, 217-228.

6 X. Hao, R. Zhang, L. He, Z. Huang and B. Wang, *Mole. Catal.*, 2018, **445**, 152-162.

7 F.-H. Wang, S.-Y. Liu, J.-X. Shang, Y.-S. Zhou, Z. Li and J. Yang, *Surf. Sci.*, 2008, **602**, 2212-2216.

8 D. N. Tafen and M. C. Gao, *JOM*, 2013, **65**, 1473-1481.

9 Y. G. Zhou, X. T. Zu, J. L. Nie and F. Gao, *Euro. Phys. J. B*, 2009, **67**, 27-34.

10 B. Hammer, *Surf. Sci.*, 2000, **459**, 323-348.

11 M. V. Ganduglia-Pirovano and M. Scheffler, *Phys. Rev. B*, 1999, **59**, 15533-15543.

12 M. Todorova, K. Reuter and M. Scheffler, *J. Phys. Chem. B*, 2004, **108**, 14477-14483.

13 Y. Xu, J. Greeley and M. Mavrikakis, *J. Am. Chem. Soc.*, 2005, **127**, 12823-12827.

14 M. Stöhr, R. Podloucky and S. Müller, *J. Phys.: Condens. Mat.*, 2009, **21**, 134017.

15 W. P. Krekelberg, J. Greeley and M. Mavrikakis, *J. Phys. Chem. B*, 2004, **108**, 987-994.

16 T. Xue, C. Wu, X. Ding and J. Sun, *Phys. Chem. Chem. Phys.*, 2018, **20**, 17927-17933.

17 A. D. Daigle and J. J. BelBruno, *Surf. Sci.*, 2011, **605**, 1313-1319.